Quasinormal mode characterization of evaporating mini black holes

Elcio Abdalla, Cecilia B. M. H. Chirenti
Instituto de Física, Universidade de São Paulo, C.P. 66318, 05315-970 - São Paulo, SP, Brazil

Alberto Saa
Departamento de Matemática Aplicada, IMECC – UNICAMP, C.P. 6065, 13083-859 - Campinas, SP, Brazil

(Dated: March 14, 2007)

According to recent theoretical developments, it might be possible to produce mini black holes in the high energy experiments in the LHC at CERN. We propose here a model based on the n-dimensional Vaidya metric in double null coordinates for these decaying black holes. The associated quasinormal modes are considered. It is shown that only in the very last instants of the evaporation process the stationary regime for the quasinormal modes is broken, implying specific, and perhaps also observable, power spectra for the perturbations around these mini black-holes. From scattered electromagnetic fields one could recover the black hole parameters as well as the number of extra dimensions. The still mysterious final fate of such objects should not alter significantly our main conclusions.

PACS numbers: 04.70.Dy, 11.25.Wx, 04.50+h, 04.30.Nk

New models with extra dimensions[1] predict the production of mini black holes in particle accelerators with sufficient large energies. Such events are expected to be obtained in the LHC at CERN[2]. These n-dimensional mini black holes are expected to be highly interacting, and, once formed, Hawking radiation[3] is expected to settle after possible transient stages. Their phenomenological and observational consequences have been intensively discussed. (See [4] for recent reviews). In particular, it is expected that their net radiated power, and hence, their mass decreasing rate, be driven by the n-dimensional Stefan-Boltzmann law[5], leading to

$$\frac{d}{dt}\left(\frac{m}{M_{\rm P}}\right) = -\frac{a_n}{t_{\rm P}}\left(\frac{m}{M_{\rm P}}\right)^{-\frac{2}{n-3}}, \qquad (1)$$

where $t_{\rm P}$ and $M_{\rm P}$ stand for the Planck time and mass, respectively, while a_n is the effective n-dimensional Stefan-Boltzmann constant[5], which depends on the available emission channels for the Hawking radiation[6]. Typically, however, one should expect $a_n \approx 10^{-3}$. Eq. (1) can be immediately integrated,

$$m(t) = m_0\left(1 - \frac{t}{t_0}\right)^{\frac{n-3}{n-1}}, \qquad (2)$$

$0 \leq t \leq t_0$, where the lifetime t_0 of a black hole with initial mass m_0 is given by

$$t_0 = \frac{n-3}{n-1}\left(\frac{m_0}{M_{\rm P}}\right)^{\frac{n-1}{n-3}}\frac{t_{\rm P}}{a_n}. \qquad (3)$$

Following Arkani-Hamed *et al*[1], the phenomenology of such mini LHC black holes can be studied by setting the Planck scale in order to have $M_{\rm P} \approx 1$TeV.

We recall that (1) is not expected to be valid in the very final stages of the black hole evaporation, where the appearance of new emission channels for Hawking radiation can induce changes[6] in the value of the constant a_n. Perhaps even the usual adiabatic derivation of Hawking radiations is not valid any longer[7]. We do not address these points here. We assume that the black hole evaporates obeying (2) for $0 \leq t \leq t_0$. The numerical analysis, however, requires the introduction of a regularization for the final instants of the evaporation process. Nevertheless, as we will see, our main results do not depend on such final details.

Here, we consider the quasinormal modes (QNM) associated to a radiating n-dimensional black hole with the decaying mass (2). Since the preferred emission channels for Hawking radiation correspond to massless fields, we model these evaporating mini black holes by means of an n-dimensional Vaidya metric [8, 9] in double-null coordinates[10, 11, 12]. The Vaidya metric corresponds to the solution of Einstein's equations with spherical symmetry in the presence of a radial flow of unpolarized radiation. In n-dimensional double-null coordinates $(u, v, \theta_1, \ldots, \theta_{n-2})$, it has the form

$$ds^2 = -2f(u,v)dudv + r^2(u,v)d\Omega^2_{n-2}, \qquad (4)$$

where $d\Omega^2_{n-2}$ stands for the unity $(n-2)$ dimensional sphere, and $f(u,v)$ and $r(u,v)$ are smooth non vanishing functions obeying[12]

$$f = -\partial_u r, \qquad (5)$$

$$\partial_v r = \frac{1}{2} - \frac{m(v)}{(n-3)r^{n-3}}, \qquad (6)$$

where, for the present case of an outgoing radiation field ($m' < 0$), v corresponds to the retarded time coordinate. We adopt hereafter natural unities ($t_{\rm P} = M_{\rm P} = \ell_{\rm P} = 1$).

Our choice for the mass function $m(v)$ is guided by the solution (2). Nevertheless, the final stage of a black hole evaporation is a rather subtle issue. A black hole could evaporate up to zero mass as described by (2), leaving behind an empty Minkowski-like spacetime[13] (or even a naked singularity[14]), or it could evaporate until it reaches a minimum mass, that is, turning into a massive remnant[15]. In order to circumvent these problems in the numerical analysis, we introduce a regularization for the final stage of the evaporation process. We consider the mass function

$$m(v) \;=\; \begin{cases} m_0\left(1-\frac{v}{t_0}\right)^{\frac{n-3}{n-1}}, & 0\le v<v_1<t_0, \\ A-B\tanh\rho(v-v_1), & v>v_1, \end{cases} \quad (7)$$

with $\rho>0$. The constants A, B and ρ are determined by imposing conditions for the continuity of $m(v)$ and its first derivative in $v=v_1$. Clearly, $A-B=m_{\rm F}$ is the mass of the final remnant. The regularization is effective only at the final instants of the evaporation process, $(t_0-v_1)/t_0\ll 1$, and $m_{\rm F}\ll 1$TeV. We will show that, during the major part of the evaporation process, the stationary regime for the quasinormal modes described in [16] holds, implying a specific, and perhaps observable, power spectrum for the perturbations around these mini black-holes. Besides, the perturbation power spectra should not depend significantly on the final fate of the black-hole.

We decompose a generic perturbation field ϕ as

$$\phi=\sum_{\ell m} r^{-\frac{n-2}{2}}\psi_\ell(u,v)Y_{\ell m}(\theta_1,\ldots,\theta_{n-2}), \quad (8)$$

where $Y_{\ell m}$ stands for the scalar spherical harmonics on the $(n-2)$ unity sphere, for which $\partial^2_{\Omega_{n-2}}Y_{\ell m}=-\ell(\ell+n-3)Y_{\ell m}$, where $\ell=0,1,2,\ldots$, and m denotes a set of $(n-3)$ integers $(m_1,m_2,\ldots,m_{n-3})$ satisfying $\ell\ge m_{n-3}\ge m_2\ge|m_1|$ (See [17] for a concise description of higher dimensional spherical harmonics). By using (5) and (6), the equation for ψ_ℓ reads

$$\frac{\partial^2\psi_\ell}{\partial u\partial v}+f(u,v)V(u,v)\psi_\ell=0, \quad (9)$$

where

$$V(u,v) \;=\; \frac{1}{2}\left(\frac{\ell(\ell+n-3)}{r^2}+\frac{(n-2)(n-4)}{4r^2} + \frac{(1-\sigma^2)(n-2)^2}{4r^{n-1}}m(v)\right). \quad (10)$$

The constant σ determines the type of the perturbation considered: $\sigma=0$ corresponds to scalar and gravitational tensor perturbations, $\sigma=1$ to gravitational vector perturbations, $\sigma=2/(n-2)$ to electromagnetic vector perturbations, and $\sigma=2-2/(n-2)$, finally, to electromagnetic scalar perturbations[18].

We perform an exhaustive numerical analysis of the equations (5), (6), and (9) along the same lines of the method proposed in [16]. In particular, we could verify that the QNM stationary behavior for slowly varying masses reported in [16] is not altered in higher dimensional spacetimes, see Fig. 1. Hence, provided the

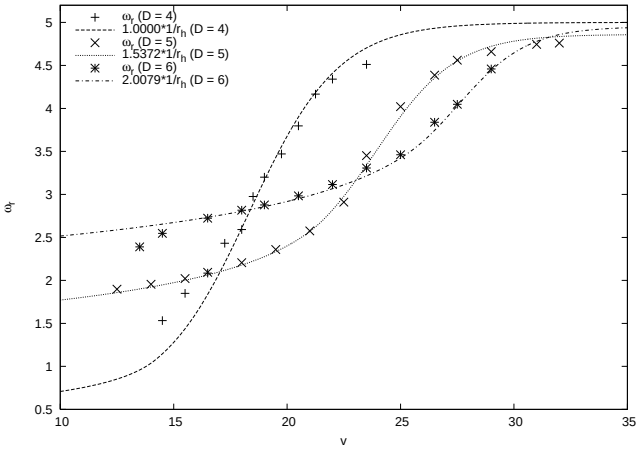

FIG. 1: QNM "instantaneous" frequencies (see [16]) for the equation (9). In the stationary regime, the frequencies follow the track corresponding to $1/r_h(v)$. The cases depicted here corresponds to $\sigma=0$, $\ell=2$, and $a=0.02$.

mass function $m(v)$ varies slowly, the QNM of (9) set down in a stationary regime, and the associated frequencies ($\tilde\omega_{\rm R}$) and damping terms ($\tilde\omega_{\rm I}$) follow the track corresponding to $1/r_h(v)$, where r_h is the horizon radius of an n-dimensional black-hole of mass m. In a more quantitative way, one has

$$\tilde\omega_{\rm R,I}(v) \;=\; \omega_{\rm R,I}\left(\frac{n-3}{2m(v)}\right)^{\frac{1}{n-3}} \;=\; \omega_{\rm R,I}\left(\frac{n-3}{2m_0}\right)^{\frac{1}{n-3}}\left(1-\frac{v}{v_0}\right)^{-\frac{1}{n-1}}, \quad (11)$$

where $\omega_{\rm R,I}$ stand for the oscillation frequency (R) and damping term (I) of the QNM corresponding to an n-dimensional Schwarzschild black hole with mass m_0. We notice that the relation $\omega_{\rm R}\propto 1/r_h$ for n-dimensional Schwarzschild black holes has been previously obtained by Konoplya in [19]. As in [16], we have used Gaussian initial conditions for all the analysis, although equivalent results can be obtained for any localized initial condition.

The condition for the QNM stationary regime is $|m''|<|\tilde\omega_{\rm I}|$, where $\tilde\omega_{\rm I}$ is the smallest damping term of the system[16]. In the present case, it reads

$$|m''(v)|<|\omega_{\rm I}|\left(\frac{n-3}{2m(v)}\right)^{\frac{1}{n-3}}, \quad (12)$$

where $\omega_{\rm I}$ is the smallest damping term of an n-dimensional Schwarzschild black hole, typically corresponding to scalar perturbations. For the mass function

(2), condition (12) reads

$$\frac{v}{t_0} < 1 - a_n^{2\frac{n-1}{n}} \left[\left(\frac{n-3}{2} \right)^{\frac{n-2}{n-3}} m_0^{\frac{n}{n-3}} |\omega_{\rm I}| \right]^{-\frac{n-1}{n}}. \quad (13)$$

For the LHC mini black holes, the term between square brackets should never exceed unity, irrespective of n. Thus, only in the very late times of the evaporation process (for typical values of a_n, for less than the last 10^{-6} fraction of the lifetime period) the stationary regime is broken. The late time exponentially suppressed perturbation of (9) will be well approximated by

$$\tilde{\psi}(v) = e^{-\tilde{\omega}_{\rm I} v} \sin\left(\tilde{\omega}_{\rm R} v + \delta\right) \quad (14)$$

for $0 \leq v < t_0$, and $\tilde{\psi}(v) = 0$ for $v \geq t_0$, where $\tilde{\omega}_{\rm R,I}$ are themselves functions of v given by (11), and δ is an arbitrary phase.

Our main observation is that, for the typical values of the parameter a_n and $m_0 \approx 1$TeV, the Fourier spectrum $\tilde{\Psi}(f)$ of the stationary perturbations (14) is very close to the the Fourier spectrum $\Psi(f)$ of the perturbations corresponding to a n-dimensional Schwarzchild case ($m(v) = m_0$),

$$\psi(v) = e^{-\omega_{\rm I} v} \sin\left(\omega_{\rm R} v + \delta\right) \quad (15)$$

for $v \geq 0$. This fact, clearly illustrated in Fig. 2, certainly would deserve a more rigorous analysis. Some simple estimations, however, do endorse the observation. From the linearity of the Fourier transform and Parseval's theorem, we have that

$$\int_0^\infty \left(\psi(v) - \tilde{\psi}(v)\right)^2 dv = \int_{-\infty}^\infty \left|\Psi(f) - \tilde{\Psi}(f)\right|^2 df. \quad (16)$$

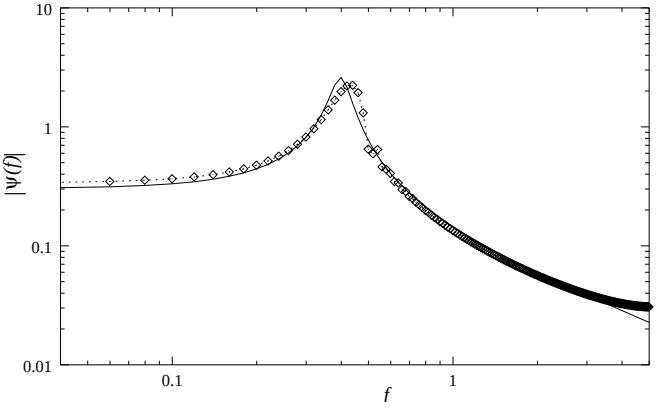

FIG. 2: The power spectra: $|\Psi(f)|$, the solid line, given by Eq. (20); and $|\tilde{\Psi}(f)|$, the line with points, calculated numerically from (14) and (11). They are indeed very close for the typical values of a and $m_0 \approx 1$TeV. In particular, both spectra exhibit similar pronounced peaks. Note that the discrepancies for large values of ω are due to the FFT aliasing effect for frequencies larger than the Nyquist critical frequency[20], and not to real differences between $|\Psi(f)|$ and $|\tilde{\Psi}(f)|$. The case depicted here corresponds to $n = 4$, $a_4 = 0.002$, $\omega_{\rm R} = 0.25$, $\omega_{\rm I} = 0.01$, and $\delta = 0$.

Hence, provided the left handed side of (16) be small, $\Psi(f)$ will be close (in the L^2 norm) to $\tilde{\Psi}(f)$. The integral in the left handed side of (16) can be split as

$$I_1 + I_2 = \int_0^{v_2} \left(\psi - \tilde{\psi}\right)^2 dv + \int_{v_2}^\infty \left(\psi - \tilde{\psi}\right)^2 dv. \quad (17)$$

The second integral can be estimated as

$$I_2 \leq 2\left(\int_{v_2}^\infty \psi^2 dv + \int_{v_2}^\infty \tilde{\psi}^2 dv\right) \leq 4\int_{v_2}^\infty e^{-2\omega_{\rm I} v} dv = 2\frac{e^{-2\omega_{\rm I} v_2}}{\omega_{\rm I}}. \quad (18)$$

Typically, $\omega_{\rm R}$ and $\omega_{\rm I}$ are of the same order (unity), while a_n is much smaller (10^{-3}). If one chooses v_2 corresponding, for instance, to 10 oscillation cycles of $\psi(v)$, the value of I_2 will be less than e^{-20}. This is the error involved in approximating the left handed side of (16) by I_1. On the other hand, during the 10 first oscillation cycles of $\psi(v)$, the variations of $\tilde{\omega}_{\rm R,I}(v)$ are of the order $1-(100/99)^{1/(n-1)}$ for black holes with initial mass $m_0 =$ 1 TeV. Hence, in the interval $[0, v_2]$, $\psi(v)$ is indeed very close to $\tilde{\psi}(v)$, implying that the left handed side of (16) is small and, finally, that $\tilde{\Psi}(f)$ is close to $\Psi(f)$.

The Fourier spectrum $\Psi(f)$ of the perturbation (15) can be easily calculated

$$\Psi(f) = \frac{1}{\sqrt{2\pi}} \int_0^\infty \psi(t) e^{-ift}\, dt = \frac{1}{\sqrt{2\pi}} \frac{\omega_{\rm R} \cos\delta + (\omega_{\rm I} + if)\sin\delta}{(\omega_{\rm R})^2 + (if + \omega_{\rm I})^2}. \quad (19)$$

The associated power spectrum

$$|\Psi(f)| = \frac{1}{\sqrt{2\pi}} \sqrt{\frac{(\omega_{\rm R}\cos\delta + \omega_{\rm I}\sin\delta)^2 + f^2 \sin^2\delta}{(\omega_{\rm R}^2 + \omega_{\rm I}^2 - f^2)^2 + 4f^2\omega_{\rm I}^2}} \quad (20)$$

has a pronounced peak (see Fig. 2) at f_{max} given by

$$\frac{f_{max}^2 - \left(\omega_{\rm R}^2 - \omega_{\rm I}^2\right)}{\left(\omega_{\rm R}^2 + \omega_{\rm I}^2\right)^2 - f_{max}^4} = g(f_{max}^2) = \frac{1}{2}\left(\frac{\sin\delta}{\omega_{\rm R}\cos\delta + \omega_{\rm I}\sin\delta}\right)^2, \quad (21)$$

from where we can conclude that

$$\sqrt{\omega_{\rm R}^2 - \omega_{\rm I}^2} \leq f_{\rm max} \leq \sqrt{\omega_{\rm R}^2 + \omega_{\rm I}^2}, \quad (22)$$

provided $|\omega_{\rm R}| > |\omega_{\rm I}|$, see Fig. 3.

The most interesting part of our results concerns the characterization of the signals that come out of the black hole probe. From the peaks in the power spectra of the perturbations around the evaporating mini black holes, one can determine $\omega_{\rm R}$ and $\omega_{\rm I}$ and, consequently, infer some of the black hole parameters as its initial mass m_0

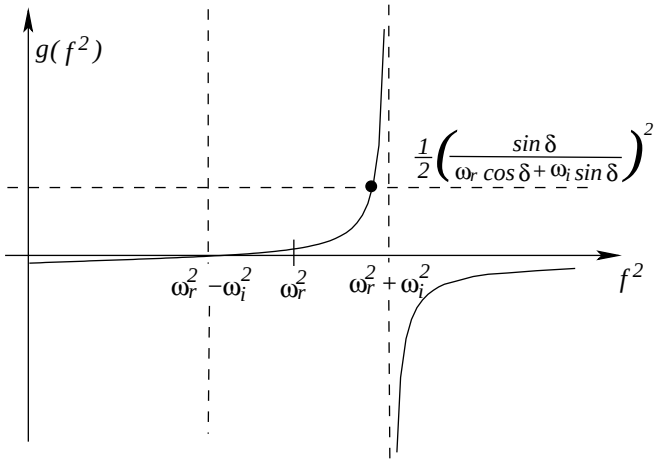

FIG. 3: Graphical solution of (21). It is clear that, for arbitrary phases δ, the peak of the power spectrum (20) is located in the range given by (22).

and even the dimension n of the spacetime where it effectively lives. We do not expect, of course, the gravitational perturbations associated to these mini black hole to be measurable. However, we remind that the QNM analysis can be applied for any test field propagating around the black hole. In particular, it also applies for real electromagnetic perturbations, and, despite these black holes emit mainly in the bulk[22], electromagnetic fields are something actually present and measurable in the LHC environment. The late time behavior of the scattering of electromagnetic waves by these evaporating mini black holes should exhibit a power spectrum as that one depicted in Fig. 2, since the electromagnetic perturbations will be also of the form (14) for large times. For instance, for 4-dimensional black holes, the QNM frequencies and damping terms for the first electromagnetic perturbations[21] are $\omega_{\rm R} = 0.2483$ and $\omega_{\rm I} = 0.0925$, implying that the frequency peak of the electromagnetic power spectrum be in the range

$$\left(\frac{m_0}{1\text{TeV}}\right)\hbar f_{max} = 230 \text{ to } 265 \text{ GeV}. \qquad (23)$$

Typically, the larger is the number of extra dimensions, the larger will be the peak frequency, even surpassing the limit of 1 TeV. However, from a precise determination of the peak location for electromagnetic perturbations, we can get the relevant parameters of the mini black hole, including the number of extra dimensions.

Acknowledgments

This work has been supported by Fundação de Amparo à Pesquisa do Estado de São Paulo (FAPESP) and Conselho Nacional de Desenvolvimento Científico e Tecnológico (CNPq), Brazil.

[1] N. Arkani-Hamed, S. Dimopoulos and G. Dvali, Phys. Lett. **429B**, 263 (1998); Phys. Rev. **D59**, 086004 (1999); I. Antoniadis, N. Arkani-Hamed, S. Dimopoulos and G. Dvali, Phys. Lett. **436B**, 257 (1998). For an explicity string realization of these scenarios, see D. Cremades, L.E. Ibanez and F. Marchesano, Nucl. Phys. **B643**, 93 (2002); C. Kokorelis, Nucl. Phys. **B677**, 115 (2004); E. Abdalla, B. Cuadros-Melgar, C. Molina, and A. Pavan, Nucl. Phys. **B752**, 40 (2006).

[2] S. Dimopoulos and G. Landsberg, Phys. Rev. Lett. **87**, 161602 (2001); Greg Landsberg Phys. Rev. Lett. **88**, 181801 (2002).

[3] S. Hawking, Comm. Math. Phys. **43**, 199 (1975)

[4] M. Cavaglia, Int. J. Mod. Phys. **A18**, 1854 (2003); P. Kanti, Int. J. Mod. Phys. **A19**, 4899 (2004); D.M. Gingrich, Int. J. Mod. Phys. **A21**, 6653 (2006).

[5] M. Cavaglia, S. Das, and R. Maartens, Class. Quantum Grav. **15**, L205 (2003).

[6] D.N. Page, Phys. Rev. **D13**, 198 (1976); 3260 (1976).

[7] I. Agullo, J. Navarro-Salas, and G.J. Olmo, Phys. Rev. Lett. **97**, 041302 (2006).

[8] P.C. Vaidya, Proc. Indian Acad. Sci.**A33**, 264 (1951); Nature **171**, 260 (1953).

[9] B.R. Iyer and C.V. Vishveshwara, Pramana **32**, 749 (1989).

[10] B. Waugh and K. Lake, *Phys. Rev. D* **34**, 2978-2984 (1986).

[11] F. Girotto and A. Saa, *Phys. Rev. D* **70**, 084014 (2004).

[12] A. Saa, *N-dimensional Vaidya metric with cosmological constant in double-null coordinates*, gr-qc/0701153.

[13] S. Sawayama, Phys. Rev. **D73**, 064024 (2006).

[14] Y. Kuroda Prog. Theor. Phys. **71**, 1422 (1984).

[15] B. Koch, M. Bleicher, S. Hossenfelder, J. High En. Phys. **0510**, 053 (2005).

[16] E. Abdalla, C.B.M.H. Chirenti, and A. Saa, Phys. Rev. **D74**, 084029 (2006).

[17] A. Chodos and E. Myers, Ann. Phys. **156**, 412 (1984).

[18] L. Crispino, A. Higuchi, and G. Matsas, Phys. Rev. **D63**, 124008 (2001).

[19] R.A. Konoplya, Phys. Rev. **D68**, 024018 (2003).

[20] W.H. Press, B.P. Flannery, S.A. Teukolsky, and W.T. Vetterling, *Numerical Recipes*, Cambridge University Press, 1992.

[21] S. Iyer, Phys. Rev. **D35**, 3632 (1987).

[22] V. Cardoso, M. Cavaglia, and L. Gualtieri, Phys. Rev. Lett. **96**, 071301 (2006), Erratum, *ibid*, 219902 (2006).